LAWRENCE LIVERMORE NATIONAL LABORATORY

UCRL-JRNL-215743

Air Gap Effects in LX-17

P. C. Souers, S. Ault, R. Avara, K. L. Bahl, R. Boat, B. Cunningham, D. Gidding, J. Janzen, D. Kuklo, R. Lee, L. Lauderbach, W. C. Weingart, B. Wu, K. Winer

September 29, 2005

Propellants, Explosives, Pyrotechnics

Air Gap Effects in LX-17

P. Clark Souers,* Stan Ault, Rex Avara, Kerry L. Bahl, Ron Boat, Bruce Cunningham, Doug Gidding, Jim Janzen, Denise Kuklo, Ron Lee , Lisa Lauderbach, W. C. Weingart, Ben Wu and Kris Winer

Lawrence Livermore National Laboratory, Livermore 94551, CA (USA)

*Corresponding author; e-mail: souers1@llnl.gov

Abstract

Three experiments done over twenty years on gaps in LX-17 are reported. For the detonation front moving parallel to the gaps, jets of gas products were seen coming from the gaps at velocities greater than the detonation velocity. A case can be made that the jet velocity increased with gap thickness but the data is scattered. For the detonation front moving transverse to the gap, time delays were seen. The delays roughly increase with gap width, going from 0-70 ns at "zero gap" to around 300 ns at 0.5 – 1 mm gap. Larger gaps of up to 6 mm width almost certainly stopped the detonation, but this was not proved. Real-time resolution of the parallel jets and determination of the actual re-detonation or failure in the transverse case needs to be done in future experiments.

Keywords: gap, crack, jets, roughness, jet velocity

1 Introduction

In commercial blasting, the effects of a gap between the explosive and the wall are well-known as the channel effect. The gas products from the explosive can be driven down the gap parallel to the explosive at velocities greater than the detonation velocity, and jet-to-detonation velocity ratios, U_j/U_s, of 1.0 to 1.9 have been reported [1,2]. A gap in an explosive is similar and, in the parallel case, has energy to drive the gas jet on both sides. Davis and Hill showed that such a jet can inflict serious damage on a metal witness plate [3]. The damage was largest for a 1/2-1 mm gap, and smaller gaps showed proportionately less damage.

Besides the detonation running parallel to a gap, it can also run transverse to it, We here summarize three unpublished experiments on both types of gaps in LX-17 (nominally 92.5% TATB, 7.5% kel-F) measured from 1983 to 2003.

2 Experimental Set-ups

There are three experimental set-ups, and the first is the *hemisphere*, shown schematically in Figure 1. The detonator was hemispherical with a radius of 6.65 mm. The booster was 1.867 g/cm^3 LX-10 (94.5% HMX/viton-A) of 15.9 mm radius. The LX-17 contained 7.67 $\pm$ 0.26% kel-F, 0.13% water and 0.056%

volatiles so that the TATB content was 92.14% [4]. The LX-17 part densities were 1.902 to 1.911 g/cm^3 with 1.905 g/cm^3 listed as a mean. All shots were fired at –54^{o}C.

The outer radius was held nearly constant at 35-36 mm with each radius at $\pm$ 0.05 mm. There were several types of air gaps, with one being shot at a time. The parallel gaps ran radially from the booster to the outside edge. The transverse gaps ran in a spherical shell with some inner thickness of LX-17 between the gap and the booster. The oblique gaps were a mixture of both of the previous types. The outer surface of the LX-17 was sprayed with aluminum silicofluoride which lights up when the shock wave hits it at more than 20 GPa [5]. A streak camera was used with a 20 mm/µs writing speed, U_W, and a 0.102 mm wide slit. Mirrors were set on each side of the explosive part so that side and top views of breakout were measured. A framing camera took static pictures every 50 ns.

Gap widths of 0.0, 0.127 and 0.254 mm were made by cutting out material so that the outer surface was always spherical. For the parallel geometry, there were three positions, at 0^o on the axis of symmetry, 40^o and 70^o. There were three oblique set-ups: one at 0^o and two start at 70^o, one running up and one down. The transverse cases used the same gap widths but also had inner thicknesses of 2, 5 and 10 mm. The gap tolerances, all measured at room temperature, were $\pm$0.0127 mm for the parallel and oblique geometries and $\pm$0.025 mm for the transverse cases. Thus, a "zero gap", made by fitting machined parts together, could have been 0.01-0.03 mm wide.

The second geometry was the *disk*, shown schematically shown in Figure 2 from the top side. The explosive was LX-17-1 at 1.906 $\pm$ 0.010 g/cm^3. The explosive disk had an overall radius of 100-101.6 mm and was 46.3 mm thick. It is not a single piece of LX-17 but consists of four pieces so that all gaps are measured with one shot. The largest piece has a keyhole shape (lower left in Figure 2) with a circular disk of 31-31.7 mm radius in the center and one quarter of the remaining outer explosive. On the reverse side of this largest part is a hole of 16.16 mm radius and 19.96 mm deep to hold a hemi-detonator and 1.865 g/cm^3 LX-10 booster.

The other three parts are toroidal quarter-sections. Each gap is shown in Figure 2 with four parallel (P1 to P4) and three transverse (T1 to T3). There were two sets of disks-one for parallel with gap widths of 0, 0.25, 0.5 and 1 mm and one for transverse with gaps of 0.25, 0.50 and 1 mm. For the parallel case, the streak camera slits were at angles shown by the dashed gray lines. For the transverse, the streak slits were across the center as shown by the solid black arrows. The parts were held together so that a 0.025 mm shim could not be fitted in between, and the gaps were machined to $\pm$ 0.051 mm.

A piece of glass with radial flow-ball marks was given a thin coat of aluminum and the glass was placed on the top of the assembly with the aluminum touching the explosive. The streak cameras look down through the glass. As the shock propagates, it first broke out in the center of the glass and the burning aluminum creates a brief but bright flash of light. As the shock propagates outward, the streak cameras recorded the light flash from the aluminum.

The third geometry, shown in Figure 3, was the *air-wedge*. A P-80 plane-wave lens lit a PBX 9404 booster, which ignited a circular block of LX-17 102 mm long with a 76 mm radius. A second disk of LX-17 of the same radius and 9.53 mm thickness leaned against the first LX-17 block with an angle of 2.3-2.9 degrees between, so that a variable-thickness wedge-shaped air gap was created. Both piezoelectric pins (which trigger in the 1 GPa range) and a streak camera were used along the back edge so that a total time to cross both the gap and the small LX-17 were obtained. A pin must have been used on the inside face where the slab connected with the initial charge. Shots X , Y and V were fired at -65^{o}C while T was fired at +63^{o}C. The LX-17 densities varied from 1.89 to 1.92 g/cm^{3}.

3 Parallel Gap Jet Velocities

The main feature of the parallel and oblique shots in the hemisphere and disk geometries were the jets, pushed out by the converging sides of the gaps. Figure 4 shows a streak camera picture of a hemisphere with the gap at 0^{o}, which is seen from the top in the center picture and by the two side mirrors. The tongue of light reaching out is the jet of high-speed gas products from the explosive. We take R as being the thickness of the LX-17 (about 19.5 mm) and t as being the time for the detonation to go this far, so that they are related by an average detonation velocity, $< U_S >$. This was measured by Bahl et. al. at a radius of 19 mm as 7.30 mm/µs; 25 mm 7.40 mm/µs and 35 mm 7.35 mm/µs [6], and we average $< U_S >$ to 7.40 mm/µs. The ratio of average detonation velocities is

$$\frac{< U_j >}{< U_S >} = \frac{1}{< U_S >} \frac{R + U_W (t_j - t)}{\frac{R}{< U_S >} + (t_j - t)} = \frac{R + U_W (t_j - t)}{R + < U_S > (t_j - t)} . \quad (1)$$

In the middle term, the numerator on the right is the total distance covered by the jet from the booster to its tip at the instant of the picture. The denominator on the right is its total time. The middle view in Figure 4 cannot be used because it looks down at the booster and may react to early light from this source. The side views and most other pictures cannot see the booster and Eq. (1) holds.

The velocity ratio is considered "averaged" because we had to assume a length for the entire process. For the disk geometry, the gap runs radially from about 32 mm to 88 mm so that R is 56 mm. Because the disk is thick, the 7.4 mm/µs detonation velocity, U_S, is seen as a phase velocity, W_S, along the gap of about

8.2 mm/μs. Eq. (1) is really measuring the ratio of phase velocities, but because it is a ratio taken at the same point, the result is the same.

The calculated U_j/U_s ratios are listed in Table 1 and give scattered numbers all larger than 1. There is reason to think that some of the parallel hemisphere streak records, eg. side mirrors at 70^o, looked too far into the gap. However, the 45^o and 70^o parallel data gives large ratios in 5 of 6 cases with center and side pictures being the same with no obvious trend evident. If we remove these six shots anyway, we find a good fit of ratio to gap width, d, of

$$< U_j > / < U_s > \approx 1.37 d^{0.057} \qquad (2)$$

so that the ratio rises from near-one for "zero" gap to 1.25 at 0.2 mm width and 1.37 at 1 mm width.

In the disk framing camera pictures, only the 0.25 mm crack was measurable given the lighting, and only three pictures of these were usable. In this 3 μs time period , the front of the jet appeared to move at about 8.6 mm/μs.

4 Transverse Gap Delay Times

For transverse gaps, the main question is how long was the detonation delayed? If the gap is large enough, did the detonation restart? Table 2 shows measured transit times for the hemispheres, where zero time is probably based on the capacitor discharge. No true fiducial was taken, so we take the shortest measured time for this to get the time differences. If the detonation travels through 10 mm of LX-17 before encountering the gap, the delay is smaller than for the 2 and 5 mm inner distances. The researchers clearly believed that the gaps were so small that the LX-17 re-detonated for both the hemispheres and disks but this was not proved. The delays roughly increase with gap width, going from 0-70 ns at "zero gap" to around 300 ns for 0.5–1 mm gaps.

The air-wedge data is listed in Table 3. The times listed are those measured on the outside face of the leaning slab as referenced to the time when the detonation crossed the knife-edge into the slab. This sets the largest detonation velocity as being 9.53 mm divided by 1.25-1.31 or 7.27-7.62 mm/μs, which is about right for LX-17.

We cannot go further without assuming some kind of velocity across the air gap. Ahrens, et. al. measured the time for detonation products from 1.6 g/cm^3 HNS to travel a distance across a vacuum [7]. The fastest products moved at 8 to 12 mm/μs as the distance increased from 100 to 800 mm. The peak of the products moved at 4-5 to 7 mm/μs at the two distances, where the detonation velocity of the HNS was 7 mm/μs. We now try both 5 and 8 mm/μs as a mean air gap velocity so that we can calculate an average wave velocity in the LX-17, which is shown in Figure 5 for sample V. The result shows numbers so far below the detonation velocity that the explosive must have failed at many places along the slab. However, the experiment itself did not determine whether failure actually occurred.

5 Roughness Measurements on PBX 9502 Fracture Surfaces

We have assumed that all gaps have perfectly smooth surfaces, but how much difference is there between gaps created by a machined surface and a crack? To find this out, some measurements were performed on pressed PBX 9502 samples using a Optimet Conoscan 3000 laser profilometer.

A computer-controlled laser scanning system fitted with a 16 mm lens was used. The listed absolute resolution for this laser-lens combination is 2 microns, however examination of the data indicates an effective resolution, with over-sampling, of better than a micron. In scanning, the instrument may be used in single scan-line mode or programmed to perform multiple scans in raster mode, thus generating a three-dimensional X-Y surface array of Z values. Trace step sizes are user selectable and as many as 7000 data points per single scan line may be generated. Following measurement, data was processed using Mountains software.

The samples on which measurements were made were machined from virgin billet-pressed PBX 9502. Fracture surfaces were produced by straining tensile specimens to failure in uni-axial tension. The strain rate during load-up was held constant at 0.01/s. Scans were performed on specimens fractured at -50 and at +50 degrees Celsius.

To check accuracy, scan-line measurements were made using a calibration block. For reference, single baseline scans of as-machined surfaces were made along the lathe-turned side of a broken tensile specimen, as well as on the parted end of a cylindrical compression sample 20 mm in diameter by 64.5 mm long. In addition, a 12 mm x 12 mm area scan was made at the sample end. Area scans and three single linear scans were performed on each of the two fracture specimens. For these scans the data density was 500 points per scan line. The linear scans were across the specimen's diameter and at 120 degrees rotation relative to one another Plots of the 3-dimensional arrays, and of the single scans (leveled to eliminate overall tilt) were made. The data was also processed to produce plots showing roughness and waviness, based on Gaussian filtering with the cutoff set at the default, 0.8 mm. The Ra (roughness) value was calculated for each scan.

Table 4 summarizes the roughness measurements. Surface finish for machined surfaces is the result of spiral or helical grooves left by the machine tool in combination with pitting caused by TATB crystals being torn from the machined surface. The cracked surfaces are 30 times greater than the machined ones. Compared to an overall gap width of perhaps 1 mm, the roughness of the cracked surfaces seems small. The difference in the warm and cold surfaces may be attributable to the fact that when this material fails in tension, if it is cold, fracturing tends to occur through the crystals. However when the material is warm, the crystals, or groups of crystals at the fracture surface tend to be pulled intact from the matrix.

6 Summary

Most of these experiments were done with a previous generation of static picture equipment and so only give a flavor of the effect of gaps. Parallel gaps need to be studied with real-time equipment that can measure the jet formation and movement. The transverse case needs better delay time measurement and a larger acceptor parts so that re-detonation or failure can be ascertained.

7 References

[1] L. V. Dubnov and L. D. Khotina, Channel Effect Mechanism in the Detonation of Condensed Explosives, *Combustion, Explosives and Shock Waves (Soviet)* **1966,** *2*, 97-104.

[2] G. Bjarnholt and U. Smedberg, On Detonation Driven Air Shocks in the Air Gap between a Charge and its Confinement, *Proceedings Eighth Symposium (International) on Detonation*, Albuquerque, NM, July 15-19, 1985, Naval Surface Weapons Center, Silver Spring, MD, pp. 1069-1079.

[3] W. C. Davis and L. G. Hill, “Joints, Cracks, Holes and Gaps in Detonating Explosives,” *Twelfth International Detonation Symposium*, San Diego, CA, August 11 - 16, 2002, pp. 220-229.

[4] Glenn W. Neff, Holston-Pantex LX-17 Formulation Comparison, Mason & Hanger-Silas Mason Co. report for LLNL SANL No. 805-034 and Process Development Endeavor No. 209, September, 1981.

[5] G. H. Bloom, Flash Threshold of Shocked Aluminum Silicofluoride, *Lawrence Livermore National Laboratory* report UCID-21259, **1987**.

[6] K. L. Bahl, R. S. Lee and R. C. Weingart, Velocity of Spherically-Diverging Detonation Waves in RX-26-AF, LX-17 and LX-10, *Shock Waves in Condensed Matter-1983* (Elsevier Science Pub, 1984), pp. 559-562.

[7] T. J. Ahrens, C. F. Allen and R. L. Kovach, Explosive Gas Blast: the Expansion of Detonation Products in Vacuum, *J. Appl. Phys.* **1971**, *42*, 815-829.

Acknowledgement

This work was performed under the auspices of the U.S. Department of Energy by the University of California, Lawrence Livermore National Laboratory under Contract No. W-7405-Eng-48.

Table 1. Jet length results for the LX-17 hemisphere and disk (bottom three) geometries. Two hemispheres are LX-10.

	Angle	gap	Jet Length, t_j - t (μs)			$\langle U_j \rangle$
	(deg)	(mm)	left	center	right	$\langle U_s \rangle$
Parallel	0	0-0.01	0	0.1	0	1.02
Hemi-	0	0.10-0.15	1.0	>1.3*	0.9	1.45
sphere	0	0.23-0.28	1.0	>1.4*	0.8	1.43
	0 (LX-10)	0.23-0.28	0.5	>1.2*	0.6	1.29
Parallel	45	0-0.01	0.6	0.9		1.38
	45	0.10-0.15	0.9	0.9		1.43
	45	0.23-0.28	0.9	0.9		1.43
Parallel	70	0-0.01	0.3	0.2		1.15
	70	0.10-0.15	1.0	1.0		1.47
	70	0.23-0.28	1.1	0.8		1.45
Oblique	0	0-0.01	0.1	0.1		1.06
Hemi-	0	0.10-0.15	0.4	0.5		1.25
sphere	0	0.23-0.28	0.4	0.4		1.22
	0 (LX-10)	0.23-0.28	0	0		1.00
Oblique	70up	0-0.01	0.1	0.1		1.06
	70up	0.10-0.15	0.4	0.5		1.25
	70up	0.23-0.28	0.5	0.6		1.29
Oblique	70down	0-0.01	0.1	0		1.03
	70down	0.10-0.15	0.5	0.2		1.20
	70down	0.23-0.28	0.6	0.4		1.27
Disk		0.20-0.30		2.05		1.28
Disk		0.46-0.56		2.31		1.31
Disk		0.97-1.07		2.80		1.36

* cannot be used for the ratio $\langle U_j \rangle / \langle U_s \rangle$

Table 2. LX-17 time delays measured with transverse air gaps. The top section contains absolute times and the bottom two sections time differences.

experiment	Gap Width (mm)	Absolute Transit Time (μs) for these Inner LX-17 Thicknesses (mm) 2	5	10
hemisphere	0.01-0.03	5.85	5.79	5.78
	0.08-0.18	5.86	5.86	5.82
	0.20-0.30	6.04	6.01	5.89
		Transit Time Difference (ns)		
hemisphere	0.01-0.03	70	10	0
	0.08-0.18	80	80	40
	0.20-0.30	260	230	110
		Streak Camera Difference (ns)		
disk	0.20-0.30	0±100		
	0.46-0.56	340±100		
	0.97-1.07	260±70		

Table 3. Measured times on the outside face of the leaning slab in the air-wedge experiment. Time zero is the moment of detonation at the connected part of the front face of the slab. Most data exists for shot V in the top section. Shots X, Y and T are summarized below.

V Gap (mm)	Total Time (μs)	V Gap (mm)	Total Time (μs)
0.00	1.31	3.31	2.00
0.30	1.35	3.81	2.12
0.80	1.42	4.32	2.26
1.30	1.54	4.83	2.42
1.80	1.66	5.08	2.54
2.30	1.76	5.32	2.65
2.81	1.88	5.82	3.04
		6.32	3.95

Gap (mm)	Total Time (μs) X	Y	T
0	1.25	1.25	1.25
1	1.46	1.44	1.48
2	1.65	1.64	1.70
3	1.84	1.80	1.93
4	2.05	2.00	2.25
4.4			2.75
5	2.32	2.29	
5.75	2.80	2.67	

Table 4. Summary of laser surface-roughness measurements.

Type of Surface	Surface Details	Average Roughness (μm)
Machined	Cylindrical surface	0.73
Machined	end of cylinder	0.56
Cracked	0.01/s; -50°C	11.8
Cracked	0.01/s; +50°C	24.2

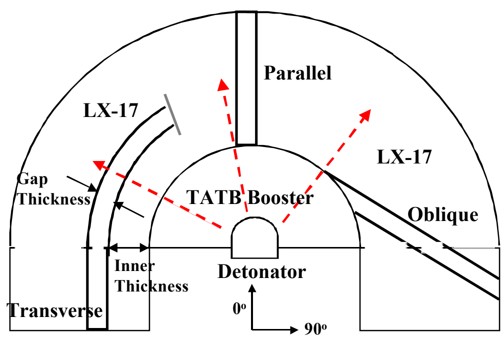

Figure 1. Schematic of the hemisphere geometry with parallel, transverse and oblique gaps shown, although only one gap was used on each actual part. The dashed lines show the direction of detonation. The axis of symmetry is 0^o.

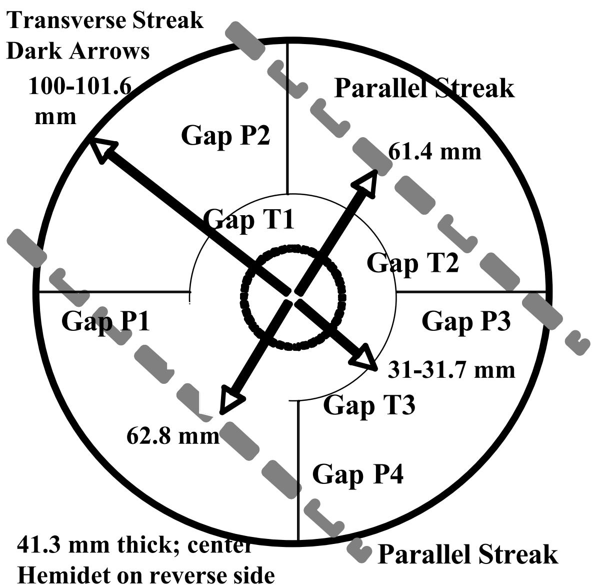

Figure 2. Schematic of the disk geometry as seen from the top. The disk is 41.3 mm thick with the detonator and booster on the back side. It consisted of the keyhole piece and three quarter-pieces. One disk was made for parallel gaps (listed P-number) and another for transverse (T-gaps). The solid arrow lines show the dimensions and where the streak slits were for the transverse shot; the gray dashed lines are the streak slits for the parallel shot.

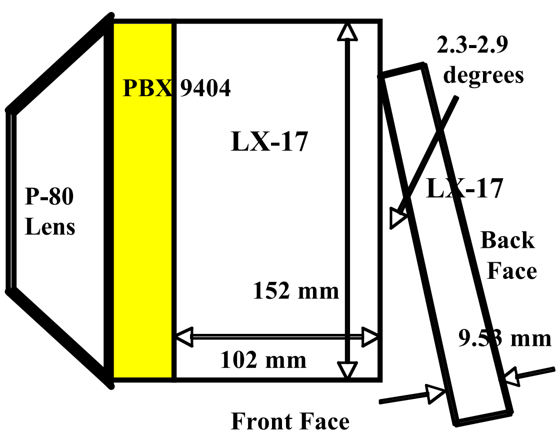

Figure 3. Schematic of the air-wedge design. A variable thickness air gap was used. The pin measurement was on the far right face of the leaning LX-17 part. A pin must have been present where the leaning part touched the main portion.

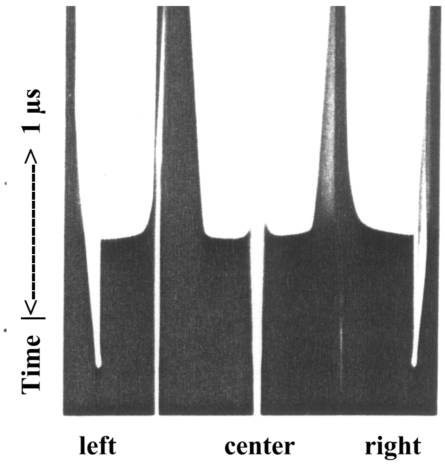

Figure 4. Streak camera view of jets in the 0^{o} parallel geometry for LX-17. The curved horizontal surfaces are the hemisphere breakout and the jets are the tongues. The 45^{o} side views give the time difference between the jet and the detonation; the center view looks clear down to the booster. The detonation moves downward.

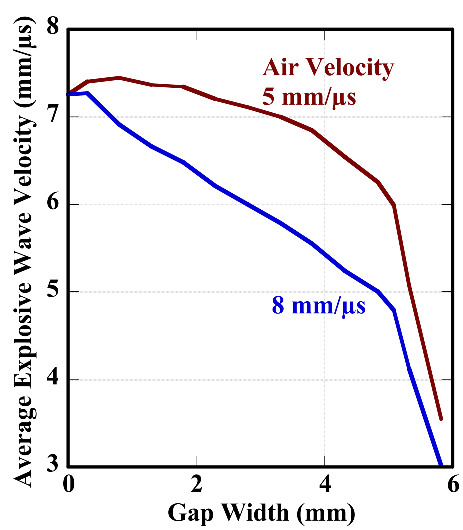

Figure 5. Calculated wave velocities for the V-shot air-wedge shot assuming the products have an average gap-crossing velocity of 5 and 8 mm/µs. Failure probably occurred for much of this but it was not proved.